

QUT Digital Repository:  
<http://eprints.qut.edu.au/>



Agha Zadeh, Ramin and Ghosh, Arindam and Ledwich, Gerard and Zare, Firuz (2009)  
***Online estimation of signal parameters in the presence of harmonic and noise distortion.*** In: 13th International European Power Electronics Conference, 8-10 September 2009, Barcelona, Spain.

© Copyright 2009 [please consult the authors]

# Online Estimation of Signal Parameters in the Presence of Harmonic and Noise Distortion

Ramin Agha Zadeh, Student Member, IEEE, Arindam Ghosh, Fellow, IEEE,  
Gerard Ledwich, Senior Member, IEEE and, Firuz Zare, Senior Member, IEEE  
Queensland University of Technology  
2 George St, GPO Box 2434, QLD, 4001  
Brisbane, Australia  
ramin.aghazadeh@qut.edu.au  
URL: <http://www.qut.edu.au>

## Acknowledgements

The authors thank the Australian Research Council (ARC) for the financial support for this project through the ARC Discovery Grant DP 0774092.

## Keywords

«Frequency estimation», «Amplitude estimation», «Phase angle estimation », «Kalman filter», «Harmonics», «Nonlinear loads».

## Abstract

An algorithm based on the concept of Kalman filtering is proposed in this paper for the estimation of signal attributes, like amplitude, frequency and phase angle. This technique can be used in protection relays, digital AVRs, DSTATCOMs, FACTS and other power electronics applications. Furthermore this algorithm is particularly suitable for the integration of distributed generation sources to power grids when fast and accurate detection of small variations of signal attributes are needed. Practical considerations such as the effect of noise, higher order harmonics, and computational issues of the algorithm are considered and tested in the paper. Several computer simulations are presented to highlight the usefulness of the proposed approach. Simulation results show that the technique can simultaneously estimate the signal attributes, even if it is highly distorted due to the presence of non-linear loads and noise.

## 1- Introduction

Control and protection of power system depend essentially on real time estimates of signal attributes. The faster and more precise are the estimates, the more reliable are the applied control and protection schemes. Harmonic and noise contamination have become a major concern for power system since it affects the accuracy of the estimates and the speed of estimation. Besides, the integration of power electronic devices to utility grids necessitates a reliable estimator not only to provide service to linear loads but also to compensate/cater for nonlinear loads. Various techniques have been introduced in the literature to measure the signal attributes. Discrete Fourier transform (DFT) and its modifications [1,2,3], Kalman filtering [4,5,6], phase locked loop (PLL) [7], least square (LS) [8,9], Newton type algorithms [10], and adaptive notch filters [11] are among the existing techniques. References [5,12-15] review these techniques and outline the drawbacks of each of them. Overall, it can be concluded that most of these techniques do not provide comprehensive estimation results including all attributes of signal (frequency, amplitude, and phase angle) for both fundamental and harmonic components. Noise and distortion sometimes affect their uniquely selective estimation process.

A literature review shows that PLL based techniques have been proved to have desirable performance in tracking the attributes of the fundamental component [12,16-19]. Reference [15] analyzes the performance of the PLL and highlights the tracking errors derived due to distortion such as phase unbalancing, harmonics, and offset. References [12,16,17] have mitigated the effects of harmonics and

noise pollution using the enhanced methods of the PLL technique. However, these techniques focus on the attributes of the fundamental component rather than other harmonic components.

Kalman-filter based techniques, extended or enhanced with frequency estimation algorithms, can provide comprehensive results comprising of the attributes of fundamental and harmonic components as well as dc-offsets [14]. Nonetheless, in order for the Kalman filter to give minimal variance of the estimation error, the statistical information about disturbances must be known a priori. The main contribution of this paper is to propose a preprocessing of the signal samples to prepare lower noise inputs to the Kalman filter. Another contribution of the paper is to propose a method to provide the Kalman filter with relatively accurate estimates of system frequency.

This paper is organized as follows. In Section 2, the proposed algorithm is derived. The development of the frequency estimation sub-algorithm and the amplitude estimation sub-algorithm are also explained in Section 2. The analysis of the proposed technique calls for some crucial parameters and relevant computation effort. The consequences of these issues and recommended solutions are explained in Section 3. Performance of the proposed method is evaluated for different conditions. Its high immunity to noise and distortion as well as its fast and accurate response to any change in the signal attributes are highlighted in Section 4. Section 5 summarizes the main conclusions of the paper.

## 2- Development of the algorithm

A power system signal is usually made up of a fundamental component plus some harmonic components and noise. Signal offset is often produced in the measurement and data conversion process using A/D devices. Therefore, a typical power system signal can be expressed as

$$y(t) = a \sin(2\pi ft) + h(t) + n(t) + v_{off}(t) \quad (1)$$

where  $a$  and  $f$  denote the amplitude and frequency of the fundamental component, respectively. Symbols  $h(t)$ ,  $n(t)$  and  $v_{off}(t)$  represent the harmonic, noise and offset parts of the signal, respectively. The signal is modeled here so that the fundamental component, the odd harmonics up to the 9<sup>th</sup> order and the offset are key parameters of the signal. However, in the proposed technique, care has been given to mitigate the effect of noise and other harmonics unaccounted for in the assumed model. The modeled signal can then be summarized as

$$y(t) = a \sin(\omega t) + \sum_{k=1}^4 a_{2k+1} \sin[(2k+1)\omega t + \theta_{2k+1}] + v_d \quad (2)$$

where  $a_k$  denotes the amplitude of the  $k^{\text{th}}$  harmonic component and  $\theta_k$  denotes the initial phase angle of the harmonic component when the phase angle of fundamental component is zero. The offset of signal in the data window of the algorithm is assumed to be taken a dc term since the data window is sufficiently small. The sampling rate chosen here is 40 kHz. This implies that in a 50 Hz cycle, 800 samples of the input signal are collected. In other words, the sampling interval is 25 $\mu$ s. In this paper  $\Delta T$  denotes this constant sampling interval.

### 2.1- Frequency estimation algorithm

The basic sub-algorithm in [14,20] called “sample counting and interpolation technique” is used here for the frequency estimation. For any two consecutive samples such as  $y_i$  and  $y_{i-1}$  where a zero crossing takes place between them, the frequency of signal is calculated as:

$$f_j = 0.5 / [(p-1)\Delta T + \alpha_j + \beta_j] \quad (3)$$

where  $p$  denotes the number of samples located between two consecutive zero crossings, the correction factors  $\alpha_j$  and  $\beta_j$  are calculated in [14] as a function of  $y_i$  and  $y_{i-1}$ . Hence,  $\alpha_j$  and  $\beta_j$  can be affected by noise as  $y_i$  and  $y_{i-1}$  used in the calculation of the correction factors are very small. Despite a threshold to lower the error imposed by noise in [14], simulation results that will be discussed in Section 4 reveal that for particular application areas such as parallel operation of UPS or DG inverters controlled by the droop method, results of frequency estimation obtained by the technique proposed in [14] is not reliable. In fact, small changes of frequency in a distorted signal, which are likely in these application areas, are too difficult for such a technique to track. Therefore, a supplementary technique to enhance the accuracy of frequency estimation results is proposed here.

Let us integrate both sides of (2) over a period of  $m\Delta T$ . This gives

$$S_i = \int_{t_i - m\Delta T}^{t_i} y(t)dt = -\frac{a}{\omega} [\cos(\omega t_i) - \cos\{\omega(t_i - m\Delta T)\}] - \frac{1}{\omega} \sum_{k=1}^4 \frac{a_{2k+1}}{2k+1} [\cos\{(2k+1)\omega t_i + \theta_{2k+1}\} - \cos\{(2k+1)\omega(t_i - m\Delta T) + \theta_{2k+1}\}] + mv_d \Delta T \quad (4)$$

Using the formula

$$\cos x - \cos y = -2 \sin\left(\frac{x+y}{2}\right) \sin\left(\frac{x-y}{2}\right) \quad (5)$$

equation (4) can be rewritten as

$$S_i = \frac{2a}{\omega} \sin\left[\omega\left(t_i - \frac{m}{2}\Delta T\right)\right] \sin\left(\frac{m\omega\Delta T}{2}\right) + \frac{2}{\omega} \sum_{k=1}^4 \frac{a_{2k+1}}{2k+1} \left\{ \sin\left[(2k+1)\omega\left(t_i - \frac{m}{2}\Delta T\right) + \theta_{2k+1}\right] \sin\left[\frac{(2k+1)m\omega\Delta T}{2}\right] \right\} + mv_d \Delta T \quad (6)$$

Let us expand the signal of (2) at  $t = t_i - m\Delta T/2$

$$y(t_i - 0.5m\Delta T) = a \sin[\omega(t_i - 0.5m\Delta T)] + \sum_{k=1}^4 a_{2k+1} \sin[(2k+1)\omega(t_i - 0.5m\Delta T) + \theta_{2k+1}] + v_d \quad (7)$$

Also let us define the following relationship

$$\frac{\sin[0.5(2k+1)m\omega\Delta T]}{(2k+1)} = \sin\left(\frac{m\omega\Delta T}{2}\right) + \frac{e_{2k+1}}{a_{2k+1} \sin[(2k+1)\omega(t_i - 0.5m\Delta T) + \theta_{2k+1}]} \quad (8)$$

where  $k = 1, \dots, 4$  and  $e_{2k+1}$  is an error parameter. The narrow sampling interval is of benefit as it produces very small errors  $e_{2k+1}$  in (8). However, we can compensate for these errors using the following equation

$$e_{2k+1} = X_i(2k+1) \{ \sin[0.5(2k+1)m\omega_{i-1}\Delta T] / (2k+1) - \sin(0.5m\omega_{i-1}\Delta T) \} \quad (9)$$

where  $X_i(2k+1)$  is related to the  $(2k+1)^{\text{th}}$  element of the process state vector,  $X$ , at  $t = t_i$ . The process state vector belongs to the Kalman filter which has been introduced in the appendix. The relevant procedure outlining the method of calculating  $X_i(2k+1)$  for different values of  $k$  is explained in the appendix and section 2. Also,  $\omega_{i-1}$  is the result of estimation for the angular frequency obtained at the previous iteration of the algorithm. It can be assumed that the system frequency does not significantly change in the very small period of  $\Delta T$  so that prior estimates can also be utilized in the following iteration.

From (6) to (9), the following equation can be obtained:

$$S_i = 2 \{ [y(t_i - 0.5m\Delta T) - v_d] \sin(0.5m\omega\Delta T) + \sum_{k=1}^4 e_{2k+1} \} / \omega + mv_d \Delta T \quad (10)$$

The integration of signal over a period of  $m\Delta T$  seconds can be approximated as:

$$S_i = \left[ \frac{y(t_i) + y(t_i - m\Delta T)}{2} + \sum_{k=1}^{m-1} y(t_i - k\Delta T) \right] \Delta T \quad (11)$$

The dc-offset, termed as  $v_d$ , has been accounted for as the eleventh element of the process estimation vector in the Kalman filter, i.e.,  $v_d$  can be obtained from the following equation:

$$v_d = X_i(11) \quad (12)$$

From (10), the following equation is derived:

$$\bar{y}_i = y(t_i - 0.5m\Delta T) - v_d = \left[ 0.5\omega_{i-1}(S_i - mv_d \Delta T) - \sum_{k=1}^4 e_{2k+1} \right] / \sin(0.5m\omega\Delta T) \quad (13)$$

Finally, the correction factors can be calculated using following condition:

$$\text{If } \bar{y}_i \times \bar{y}_{i-1} \leq 0 \text{ and } \bar{y}_{i-1} \neq 0, \text{ then } \alpha_{j+1} = \bar{y}_i \Delta T / (\bar{y}_i - \bar{y}_{i-1}) \text{ and } \beta_j = 1 - \alpha_{j+1} \quad (14)$$

Using  $\bar{y}_i$  and  $\bar{y}_{i-1}$  and instead of  $y_i$  and  $y_{i-1}$  respectively in the calculation of the correction factors,  $\alpha_{j+1}$  and  $\beta_j$  can lead to less noise sensitivity in the frequency calculation as the effect of the noise is mitigated by the summation performed in (11). Any dc-term in the signal stretches the duration of the positive half cycles of the signal, while it decreases the span of the negative half cycles. Therefore, the dc-term is subtracted from the refined signal sample in (13) so as not to undesirably raise  $\bar{y}_i$  values. The following condition can also be used to further lower the effect of noise [14]

$$\text{If } |f_j - 3/T_2| < 0.01, \text{ then } f = 3/T_2, \text{ else } f = f_j \quad (15)$$

where  $T_2$  is the time length of the latest six half cycles and  $f$  is the final result for the estimated frequency. The above-described condition implies that when the measured frequency has been almost constant for three consecutive cycles, it is better to use a longer span to calculate the frequency which will result in less error.

## 2.2- Amplitude and phase angle estimation algorithm

Let us define the following form of the signal.

$$S_i = \sum_{k=0}^{2n} y_{i-k} \quad (16)$$

where  $y_i$  is the  $i^{\text{th}}$  digital sample of  $y(t)$  defined in (2). Equation (16) can be rewritten as

$$S_i = y_{i-n} + \sum_{r=1}^n (y_{i-n-r} + y_{i-n+r}) \quad (17)$$

Let us expand the signal at  $(i-n)^{\text{th}}$  sample as follows

$$y_{i-n} = y(t_i - n\Delta T) = a_1 \sin \varphi_{i-n} + \sum_{k=1}^4 a_{2k+1} \sin [(2k+1)\varphi_{i-n} + \theta_{2k+1}] + v_d \quad (18)$$

Let us also define the following relations

$$\varphi_i = \omega_i t_i, \quad x_i = \omega_i \Delta T, \quad A_{1_i} = a_1 \sin \varphi_i, \quad A'_{1_i} = a_1 \cos \varphi_i, \quad A_{k_i} = a_k \sin (k\varphi_i + \theta_k), \quad A'_{k_i} = a_k \cos (k\varphi_i + \theta_k) \quad (19)$$

Therefore, following relation can be derived.

$$A_{k_{i+r}} = a_k \sin (k\omega t_{i+r} + \theta_k) = a_1 \sin [k\omega (t_i + r\Delta T) + \theta_k] = A_{k_i} \cos (krx) + A'_{k_i} \sin (krx) \quad (20)$$

From (18) to (20), the following equations can be obtained.

$$y_{i-n} = A_{1_{i-n}} + \sum_{k=1}^4 A_{(2k+1)_{i-n}} + v_d \quad (21)$$

$$\begin{aligned} y_{i-n-r} + y_{i-n+r} &= \left( A_{1_{i-n-r}} + \sum_{k=1}^4 A_{(2k+1)_{i-n-r}} + v_d \right) + \left( A_{1_{i-n+r}} + \sum_{k=1}^4 A_{(2k+1)_{i-n+r}} + v_d \right) = (A_{1_{i-n-r}} + A_{1_{i-n+r}}) \\ &+ \sum_{k=1}^4 (A_{(2k+1)_{i-n-r}} + A_{(2k+1)_{i-n+r}}) + 2v_d = 2A_{1_{i-n}} \cos (rx) + \sum_{k=1}^4 \left\{ 2A_{(2k+1)_{i-n}} \cos [(2k+1)rx] \right\} + 2v_d \end{aligned} \quad (22)$$

From (17), (21) and (22) the following equation is obtained.

$$\begin{aligned} S_i &= A_{1_{i-n}} + \sum_{k=1}^4 A_{(2k+1)_{i-n}} + v_d + 2A_{1_{i-n}} \sum_{r=1}^n \cos (rx) + \sum_{r=1}^n \sum_{k=1}^4 \left\{ 2A_{(2k+1)_{i-n}} \cos [(2k+1)rx] \right\} + 2nv_d \\ &= A_{1_{i-n}} \left( 1 + 2 \sum_{r=1}^n \cos (rx) \right) + (2n+1)v_d + \sum_{k=1}^4 \left\{ A_{(2k+1)_{i-n}} \left[ 1 + 2 \sum_{r=1}^n \cos [(2k+1)rx] \right] \right\} \end{aligned} \quad (23)$$

Let us define the following relation.

$$\lambda_k = 1 + 2 \sum_{r=1}^n \cos (krx) \quad (24)$$

Therefore, (23) can be rewritten as

$$S_i = \lambda_1 A_{1_{i-n}} + \sum_{k=1}^4 \lambda_{2k+1} A_{(2k+1)_{i-n}} + (2n+1)v_d \quad (25)$$

In the followings, it is proven that the Kalman filter relationship is valid for the signal of (25). Moreover, the exact relations and formula needed to obtain the parameters of the original signal will be figured out through the following math work.

Let us define an  $11 \times 1$  vector in the following manner

$$X_i(m,1) = \begin{cases} \lambda_{m_i} A'_{m_{i-n}} & m = 1, 3, 5, 7, 9 \\ \lambda_{(m-1)_i} A_{(m-1)_{i-n}} & m = 2, 4, 6, 8, 10 \\ (2n+1)v_d & m = 11 \end{cases} \quad (26)$$

It can be assumed that the frequency does not change considerably in a small duration of  $\Delta T$ . Thus,

$$\omega_{i+1} = \omega_i \Rightarrow \lambda_{m_{i+1}} = \lambda_{m_i} \quad (27)$$

From (19), (26) and (27) the following equation is derived.

$$\begin{aligned} \lambda_{(2k-1)_{i+1}} A'_{(2k-1)_{i-n+1}} &= \lambda_{(2k-1)_i} a_{(2k-1)} \cos[(2k-1)(\varphi_{i-n} + x)] \\ &= \lambda_{(2k-1)_i} A'_{(2k-1)_{i-n}} \cos[(2k-1)x] - \lambda_{(2k-1)_i} A_{(2k-1)_{i-n}} \sin[(2k-1)x] \end{aligned} \quad (28)$$

$$\begin{aligned} \lambda_{(2k-1)_{i+1}} A_{(2k-1)_{i-n+1}} &= \lambda_{(2k-1)_i} a_{(2k-1)} \sin[(2k-1)(\varphi_{i-n} + x)] \\ &= \lambda_{(2k-1)_i} A_{(2k-1)_{i-n}} \cos[(2k-1)x] + \lambda_{(2k-1)_i} A'_{(2k-1)_{i-n}} \sin[(2k-1)x] \end{aligned} \quad (29)$$

From (28) and (29) the following equation is derived.

$$\begin{bmatrix} \lambda_{(2k-1)_{i+1}} A'_{(2k-1)_{i-n+1}} \\ \lambda_{(2k-1)_{i+1}} A_{(2k-1)_{i-n+1}} \end{bmatrix} = \begin{bmatrix} \cos[(2k-1)x] & -\sin[(2k-1)x] \\ \sin[(2k-1)x] & \cos[(2k-1)x] \end{bmatrix} \begin{bmatrix} \lambda_{(2k-1)_i} A'_{(2k-1)_{i-n}} \\ \lambda_{(2k-1)_i} A_{(2k-1)_{i-n}} \end{bmatrix} = f[(2k-1)x] \begin{bmatrix} \lambda_{(2k-1)_i} A'_{(2k-1)_{i-n}} \\ \lambda_{(2k-1)_i} A_{(2k-1)_{i-n}} \end{bmatrix} \quad (30)$$

From (26) and (30) the following equation can be derived.

$$X_{i+1} = \text{diag} \cdot [f(x), f(3x), f(5x), f(7x), f(9x), 1] X_i \quad (31)$$

where  $\text{diag} \cdot$  denotes the diagonal elements of a square matrix.

Equations (30) and (31) reveal that  $X$  can be deemed as a process state vector of a Kalman filter. The Appendix describes briefly the details of Kalman filter.  $H$ , the connection matrix between the measurement vector and state-process vector of Kalman filter, can be arranged in the following manner to make the processed signal,  $S(t)$ , a suitable input for the Kalman filter.

$$Z_i = H X_i = [0, 1, 0, 1, 0, 1, 0, 1, 0, 1, 1] X_i = \lambda_{1_i} A_{1_{i-n}} + \lambda_{3_i} A_{3_{i-n}} + \lambda_{5_i} A_{5_{i-n}} + \lambda_{7_i} A_{7_{i-n}} + \lambda_{9_i} A_{9_{i-n}} + (2n+1)v_d = S_i \quad (32)$$

Let us define another  $11 \times 1$  vector with the elements specified as follows

$$Y_i(m,1) = \begin{cases} A'_{m_{i-n}} & m = 1, 3, 5, 7, 9 \\ A_{(m-1)_{i-n}} & m = 2, 4, 6, 8, 10 \\ v_d & m = 11 \end{cases} \quad (33)$$

Definitions (26) and (33) can give:

$$Y = D X \quad (34)$$

$$\text{where } D = \text{diag} \cdot [\lambda_1^{-1}, \lambda_1^{-1}, \lambda_3^{-1}, \lambda_3^{-1}, \lambda_5^{-1}, \lambda_5^{-1}, \lambda_7^{-1}, \lambda_7^{-1}, \lambda_9^{-1}, \lambda_9^{-1}, (2n+1)^{-1}] \quad (35)$$

The amplitude,  $a_k$  and phase angle,  $\psi_k$  of the signal components can be calculated as

$$a_{k_i} = \sqrt{Y_i^2(k,1) + Y_i^2(k+1,1)} \quad (36)$$

$$\psi_{k_i} = k\varphi_i + \theta_k = \begin{cases} \eta_{k_i} & Y_i(k,1) \geq 0, Y(k+1,1) \geq 0 \\ \eta_{k_i} + 2\pi & Y_i(k,1) \geq 0, Y(k+1,1) < 0 \\ \eta_{k_i} + \pi & \text{else} \end{cases} \quad (37)$$

where  $k = 1, 3, 5, 7, 9$  and  $\eta_k$  is given by

$$\eta_{k_i} = \text{tg}^{-1} \left( \frac{Y_i(k+1,1)}{Y_i(k,1)} \right) + nx \quad (38)$$

The term “ $nx$ ” is intended to compensate for the delay imposed by performing the summation in (17). The offset part can also be extracted from the following equation.

$$(v_d)_i = Y_i(11,1) \quad (39)$$

### 3- Discussion on the choice of parameters and computational issues

There are a number of parameters that should be considered in the development of the proposed algorithm. In this section what these parameters are and how they should be defined or modeled are being discussed.

#### 3.1- Parameter $m$

The larger is the parameter  $m$ , the less is the effect of noise and distortion on the estimates of

frequency, albeit at the expense of a longer delay in obtaining the estimates. Hence, a compromise is made to obtain an optimal setting. Simulation tests, carried out for a wide range of variation of this parameter, reveal that  $m=40$  could be a good solution while dealing with such a high setting for the sampling frequency. Accordingly, the imposed delay in zero-crossing detection resultant from integration process in (4) and (11) is about  $m\Delta T/2$  or 0.5ms.

### 3.2- Parameter $n$

The term,  $2n+1$ , indicates the number of samples that are being summed in (17). The larger is  $n$ , the less is the error imposed by noise and unaccounted-for harmonics on the estimates, albeit at the expense of a longer delay. In this study,  $n$  is chosen 40 so that 81 consecutive samples are being summed up in (17). Thereby, summing up across a period of  $80\Delta T$ , which is actually one tenth of the nominally fundamental period of the signal, implements a digital low-pass filter whose cut-off frequency is about 500Hz. Therefore, some negative effects of both noise and harmonics higher than the tenth order can be mitigated.

### 3.3- Noise parameters

A random noise with zero mean and Gaussian distribution with  $0.02pu$  of standard deviation is the typical model of noise used in the simulations of this paper. This signal conventionally models the noise related to the measurement and signal conversion in A/D. Furthermore, an unconventional noise which relates to the high frequency sampling rate of A/Ds is also applied. In spite of reliable clocks and accurate counters used by microprocessors to define the exact instant of performing the sampling subroutines, in practice a variable, slight time delay due to internal loading of microprocessors and the internal hardwired interfaces of the system exists for an A/D to receive the sampling command. Also, a variable delay depending upon the quality of A/D and its speed in high frequency ranges must be supposed for the A/D to take the samples right after receiving the command. Therefore, the sampling interval in the simulations has been supposed to be a random signal with 40-kHz mean and Gaussian distribution of 2.1% standard deviation.

Moreover, the load variation, which can affect the amplitude of current signal and even the amplitude of voltage signal in case of a weak source, can be modeled as a random noise. Therefore, a random signal of Gaussian distribution with zero mean and  $0.02pu$  of standard deviation has been set for the variant part of the signal amplitude in the simulations.

### 3.4- Computational load on microprocessor

Three methods are proposed here to lower the computational load on the microprocessor. The first method involves storing some matrices in the offline mode and retrieving them for the on-line computations. Matrices  $D$  in (35) and  $F$ , the state transition matrix defined in the Appendix in (48) can be sorted by frequency and stored consecutively in the memory of microprocessor.

The second method recommends that sampled data are logged until the microprocessor becomes free to process them. In this case, the highest priority of the microprocessor's interrupt services will be allocated for the subroutine that exerts the zero-crossing detection based on the idea proposed as per (11) to (14). As soon as a new sample is received from A/D, it will be used to update (11) and examine the zero crossing condition in (14) to find out whether or not the frequency estimation needs to be updated. The lower priorities are being allocated for performing other normal routines and computations. Meanwhile, if any fresh sample arrives in the middle of processing older samples, it will be logged for the next course of computation, of course after it is being examined by the interrupt service routine of zero-crossing detection.

The third solution proposes the idea of producing the Kalman gains and error covariance matrices in the offline mode and save them in the memory of the microprocessor. In the philosophy of Kalman filtering, these two are supposed to be developed in a recursive manner which does not leave a chance to somehow store their real series in a memory with a limited capacity. However, the Kalman gains as well as the error covariance matrices can be sequentially chosen from a set of confined periodic data. In fact, for a Kalman filter it can take less than one period of its input signal, to approach the target, defined as sine, cosine or offset components constituting the real signal. To constitute the appropriate set of data necessary to allocate for the Kalman gains and the error covariance matrices, the initial effort is to produce these data recursively starting from the initial information, specified by (55) and (63) in the Appendix, and ending at least at the 817<sup>th</sup> iteration. This can make sure that there will be enough data stored to support a whole cycle even for the longest possible signal which is assumed to have the frequency of 49Hz.

## 4- Simulation studies

In this section, the proposed algorithm is tested for various simulated signals. Appropriate software codes to generate the test signals as well as to develop the main algorithm are coded in MATLAB. The performance of the proposed technique is highlighted below.

### 4.1- Change of frequency

The test signal with the following characteristics is applied to test the ability of the proposed technique in frequency estimation.

$$\begin{aligned}
 y(t) = & [1 + n_1(t)] \sin(\omega t) + [0.07 + n_2(t)] \sin(3\omega t + \frac{\pi}{6}) + [0.05 + n_3(t)] \sin(5\omega t + \frac{\pi}{5}) \\
 & + [0.04 + n_4(t)] \sin(7\omega t + \frac{\pi}{4}) + [0.03 + n_5(t)] \sin(9\omega t + \frac{\pi}{10}) + [0.02 + n_6(t)] \sin(11\omega t + \frac{\pi}{20}) \\
 & + [0.01 + n_7(t)] \sin(13\omega t + \frac{\pi}{18}) + [0.025 + n_8(t)] \sin(15\omega t + \frac{\pi}{20}) + 0.1 + n(t)
 \end{aligned} \quad (40)$$

where  $n_k(t)$  for  $k=1,2,\dots,8$  are random noise signals with zero mean and a standard deviation of 2 percent of the amplitude of the component. These noises are intended to simulate the random changes in the customer load. The offset of  $0.1pu$ , in conjunction with  $n(t)$ , a random noise with zero mean and  $0.02pu$  standard deviation, has been added to simulate low frequency and measurement noise, respectively. Furthermore, the sampling interval is supposed to be randomly variant because of its high frequency rate. As mentioned before, applied sampling interval is a random signal with a 40kHz mean and a standard deviation of 2.1 percent.

The test signal experiences a sudden drop of frequency at  $t=500ms$ . The frequency changes from 50Hz to 49.97Hz to simulate switching on of a considerable load to the power system which can take place particularly in integrated DGs or Micro-grids controlled through the droop-method. Fig. 1.a shows the performance of the algorithm in this case where the proposed method (solid-line) is compared with the method of [14] (dotted line). The actual frequency changes are also shown in this figure through the dashed line. It should be noted that the technique proposed in [14], despite taking care of the noise, can not properly detect the actual changes of frequency in such a distorted signal. However, the supplementary techniques proposed in this paper have improved the performance in tracking the frequency changes in spite of high disturbances. Fig. 1.b shows the results of amplitude estimation by the proposed technique. The results for the amplitude estimates of the third up to the ninth harmonics have been 10 times scaled up for better presentation. As shown in this figure, the frequency change has no negative side effects on the amplitude estimates of the proposed technique.

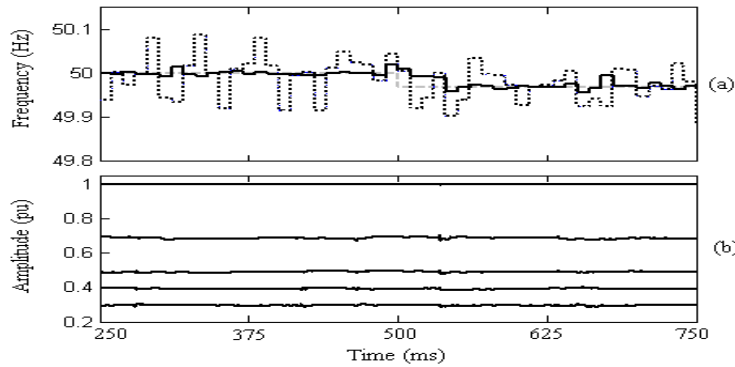


Fig. 1. (a) Response to a step change in frequency: solid line: the proposed method, dotted-line: the method of [14] and dashed-line: the actual frequency changes. (b) Amplitude estimates in case of frequency change

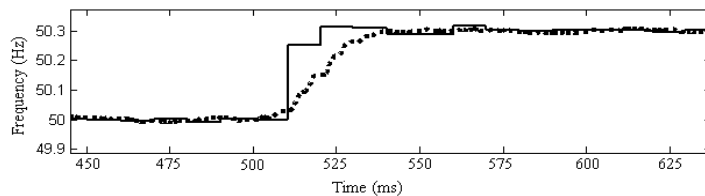


Fig. 2. Response to a step change in frequency: solid line: proposed method, dotted-line: the phasor measurement method [2]

Fig. 2 shows the response of the proposed algorithm to a frequency change of +0.3Hz where the proposed method (solid-line) is compared with the phasor measurement method proposed in [2] (dotted line). As shown in Fig. 2, a delay of 2 cycles is unavoidable for the phasor measurement technique to track the frequency when the signal is distorted especially by low frequency noises. However, the proposed technique can track the frequency of the same signal within 2/3 of a cycle.

#### 4.2- Change of amplitude and phase angle

In this case, the test signal polluted with noise, offset and unaccounted-for harmonics encounters a sudden phase angle changes for the components of the signal at  $t=400ms$ . In the following equations,  $y_1(t)$  and  $y_2(t)$  are respectively the applied test signals before and after  $t=400ms$  until  $t=700ms$ . In addition, the amplitude of the fundamental component in  $y_2(t)$  also drops suddenly from  $1pu$  to  $0.95pu$  at  $t=700ms$ .

$$\begin{aligned}
 y_1(t) = & [1 + n_1(t)] \sin(\omega t) + [0.07 + n_2(t)] \sin(3\omega t + \frac{\pi}{12}) + [0.05 + n_3(t)] \sin(5\omega t + \frac{7\pi}{36}) \\
 & + [0.04 + n_4(t)] \sin(7\omega t + \frac{5\pi}{18}) + [0.03 + n_5(t)] \sin(9\omega t + \frac{\pi}{3}) + [0.02 + n_6(t)] \sin(11\omega t + \frac{\pi}{20}) \\
 & + [0.01 + n_7(t)] \sin(13\omega t + \frac{\pi}{18}) + [0.025 + n_8(t)] \sin(15\omega t + \frac{\pi}{20}) + 0.1 + n(t)
 \end{aligned} \tag{41}$$

$$\begin{aligned}
 y_2(t) = & [1 + n_1(t)] \sin(\omega t + \frac{\pi}{18}) + [0.07 + n_2(t)] \sin(3\omega t + \frac{\pi}{6}) + [0.05 + n_3(t)] \sin(5\omega t + \frac{\pi}{4}) \\
 & + [0.04 + n_4(t)] \sin(7\omega t + \frac{11\pi}{36}) + [0.03 + n_5(t)] \sin(9\omega t + \frac{4\pi}{9}) + [0.02 + n_6(t)] \sin(11\omega t + \frac{\pi}{6}) \\
 & + [0.01 + n_7(t)] \sin(13\omega t + \frac{2\pi}{9}) + [0.025 + n_8(t)] \sin(15\omega t + \frac{\pi}{5}) + 0.1 + n(t)
 \end{aligned} \tag{42}$$

Fig. 3(a) shows the results of amplitude estimation process of the proposed technique. The results for the amplitude estimates of the third up to the ninth order harmonics have been 10 times scaled up for better presentation. Although a lot of noise and pollution have distorted the input signal, significantly accurate results are obtained. Error of estimation in the amplitude estimates due to the distortion is always less than one percent. However, the amplitude estimation is moderately affected at  $t=400ms$  due to the catastrophic changes in the phase angles of signal components. The algorithm also tracks successfully the sudden change in the amplitude of the fundamental component at  $t=700ms$  and then converges to the new target in less than a cycle without any substantial side effects on the estimates of the other attributes of the signal.

Fig. 3(b) shows the results of estimation for the phase angles of the components of the signal from fundamental to the ninth order harmonic. For ease of presentation, the difference between the estimated phase angles of any component and its actual phase part of  $k\omega t$  (where  $k$  is the harmonic order) has been utilized. The results have also been prepared in degrees.

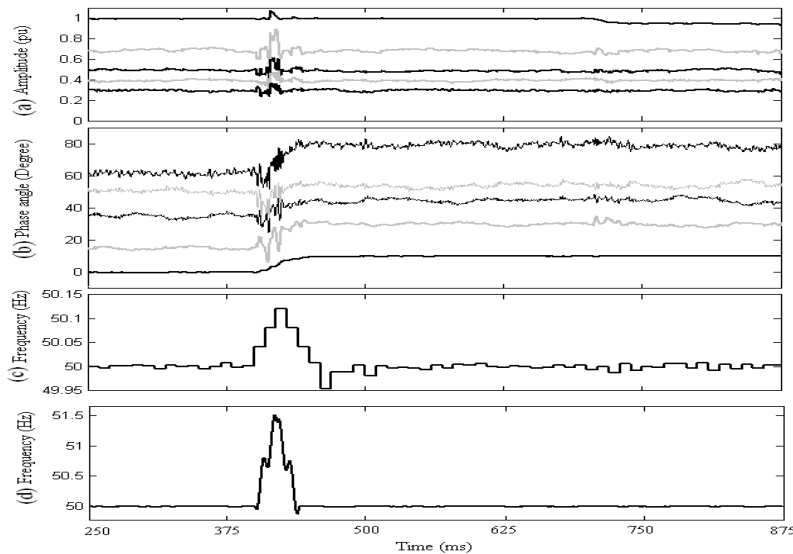


Fig. 3 Response to step changes in phase angle and amplitude

The best accuracy in the results belongs to the fundamental component so that the error is less than  $0.15^\circ$ . At the same time, the worst estimates belong to the ninth order harmonic with errors up to 4 degrees in this regard. As shown in Fig. 3(b), the convergence of the algorithm to the new targets after a sudden phase angle change happens in less than a cycle. Fig. 3(c) shows the frequency estimation result in this simulation test. The result is satisfactorily accurate and reliable despite a transient side effect due to the catastrophic angle changes at  $t=400ms$ . As shown in Fig. 3(c), the frequency estimate is relatively robust against sudden or even random changes of amplitude. Fig. 3(d) shows the response of the phasor measurement method [2] to the same signal. The transient error due to the sudden phase angle change is catastrophic and the results can lead to an undesirable trip or a failure in the control and protection of power system. The error in the transient state from the proposed technique, 0.12Hz as per Fig. 3(c), is much less than that of the phasor measurement technique, 1.5Hz as per Fig. 3(d). The results of further simulations show that the transient error of the phasor measurement technique in response to sudden phase angle changes can be higher depending upon the amount of change, the point at which the change happens, and the component/components to which the change is applied.

### 4.3- Simultaneous change in frequency and amplitude

In particular application areas such as parallel operation of DG inverters, frequency and amplitude are subjected to simultaneous changes. As load sharing is usually controlled based on the droop method, load changes lead to droop or rise in both amplitude and frequency of voltage and current signals. In the following test, the same signal as described in (40) is utilized for the simulation but at  $t=500ms$  the frequency changes suddenly from 50Hz to 50.05Hz and simultaneously the amplitudes of components change, too. The amplitude of the fundamental component increases from  $1pu$  to  $1.05pu$  and the amplitudes of the other components increase by 10 percent. Fig. 4 shows the result of frequency and amplitude as well as offset estimations. For better presentation, the results of amplitude estimates for the third up to the ninth harmonics have been scaled up for 10 times. The offset has been shown in dotted-style graph. Despite the large changes, the algorithm effectively tracks the signal attributes. In this case, the steady state error of frequency estimates is less than 0.008Hz. Besides, the error of amplitude estimation is less than  $\pm 1\%$ .

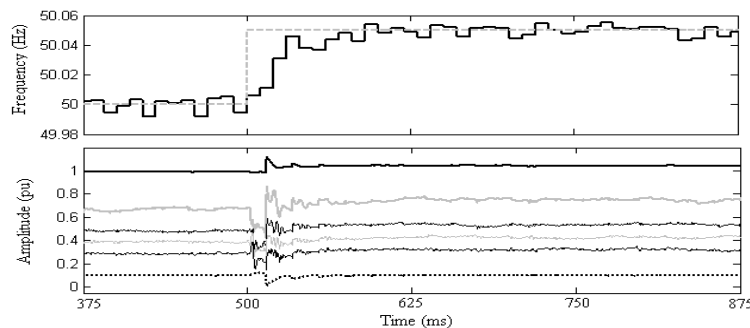


Fig. 4 Response to simultaneous change in frequency and amplitude

## 5- Conclusion

A new technique is proposed for the estimation of signal attributes and its performance is evaluated. The method is based on the Kalman filter to provide comprehensive estimates. The drawbacks of the Kalman filter related to its sensitivity to the information about the disturbances, has been improved by providing preprocessed inputs to the Kalman filter. In this regard, firstly the system frequency is estimated accurately to be fed to the Kalman filter. Secondly, samples are pre-filtered by a simple FIR filter before being processed by the Kalman filter. This pre-filtering mitigates noise and harmonic pollution effects. The results obtained from various simulation studies demonstrate the effectiveness of the proposed technique.

## Appendix

The Kalman filtering basic theory and model development is described here. More detailed theory can be found in standard text books [21,22].

The design of a Kalman filter requires a state-space model of the signal to be estimated in the form of:

$$X_{i+1} = FX_i + N_i \quad (43)$$

$$Z_i = HX_i + M_i \quad (44)$$

where  $X_i$  is an  $n \times 1$  process state vector at time  $t_i$ ,  $F$  is an  $n \times n$  state transition matrix,  $N_i$  is an  $n \times 1$  noise vector—assumed to be a white sequence with known covariance matrix  $Q$ ,  $Z_i$  is an  $m \times 1$  measurement vector at  $t_i$ ,  $H$  is an  $m \times n$  matrix giving the noiseless connection between the measurement and the state vector,  $M_i$  is an  $m \times 1$  measurement error vector—assumed to be a white noise sequence with known covariance matrix  $R$  and uncorrelated with  $N_i$  sequence,  $n$  represents the order of system and  $m$  represents the number of outputs being measured.

The covariance matrices for  $N_i$  and  $M_i$  vectors are given as follow:

$$E[N_i N_j^T] = \begin{cases} Q & i = j \\ 0 & i \neq j \end{cases} \quad E[M_i M_j^T] = \begin{cases} R & i = j \\ 0 & i \neq j \end{cases} \quad (45)$$

where  $E$  denotes the expected value. Having the prior knowledge of initial estimation error covariance matrix  $P_0^-$ , the Kalman gains can be computed recursively as follows.

$$K_i = P_i^- H^T (HP_i^- H^T + R)^{-1}, \quad P_i = (I - K_i H) P_i^-, \quad P_{i+1}^- = FP_i F^T + Q \quad (46)$$

where  $K_i$  is the Kalman gain matrix at time  $t_i$ ,  $P_i^-$  is the estimation error covariance matrix at time  $t_i$ ,  $P_i$  is the error covariance matrix for the updated estimate at time  $t_i$ ,  $I$  denotes the identity matrix.

Having an initial state estimate,  $\hat{X}_0^-$ , the Kalman filter equation, which recursively estimates new values of the state vector, is as follows.

$$\hat{X}_i = \hat{X}_i^- + K_i (Z_i - H\hat{X}_i^-) \quad \hat{X}_{i+1}^- = F\hat{X}_i \quad (47)$$

where  $\hat{X}_i$  is the estimate of  $X_i$ . The discrete-time state-space representation of a periodic signal having odd harmonic components up to  $(2k-1)^{\text{th}}$  order with samples  $Z_i$  at time  $t_i$  is given as (47), where  $X_i$  is a  $(2k+1)$  state vector and

$$F = \text{diag} [f(x), f(3x), f(5x), \dots, 1] \quad (48)$$

where  $\text{diag}$ . denotes the diagonal elements of a square matrix and  $x = \omega\Delta T$ . The matrix function  $f$  and the connection matrix  $H$  is stated as follow.

$$f[(2k-1)x] = \begin{bmatrix} \cos[(2k-1)x] & -\sin[(2k-1)x] \\ \sin[(2k-1)x] & \cos[(2k-1)x] \end{bmatrix} \quad H = [1, 0, 1, 0, 1, 0, 1, 0, 1] \quad (49)$$

The amplitudes and the phase angles of the components are given by:

$$h_i^2(2k-1) = X_i^2(2k-1) + X_i^2(2k) \quad \phi_i(2k-1) = \begin{cases} \psi_i(2k-1) & X_i(2k) \geq 0, X_i(2k-1) \geq 0 \\ \psi_i(2k-1) + \pi & X_i(2k) < 0 \\ \psi_i(2k-1) + 2\pi & X_i(2k) \geq 0, X_i(2k-1) < 0 \end{cases} \quad (50)$$

$$\text{where } \psi_i(2k-1) = \text{tg}^{-1}[X_i(2k-1)/X_i(2k)] \quad (51)$$

In order to find the matrices  $R$  and  $P_0^-$ , it is required to have the information of the signal. For the proposed method, the statistical matrices can be obtained by the following manner.

Since, the random load changes are supposed to be modeled as a Gaussian noise with zero mean and  $0.02pu$  of standard deviation, it can be assumed that the amplitudes of signal components can vary with  $0.02pu$  of standard deviation. Therefore, from (48) and (50), the covariance matrix  $Q$  can be obtained as

$$Q = \sigma_N^2 = 0.02^2 = 0.0004 \text{ pu}^2 \quad (52)$$

where  $\sigma_N$  is the standard deviation of  $N_i$  that originates from random load changes.

The measurement error for true samples of the signal, simulated by  $n(t)$ , is supposed to be a Gaussian noise with zero mean and  $0.02pu$  of standard deviation. Thus, we get

$$\text{Var}(y) = 0.02^2 = 0.0004 \text{ pu}^2 \Rightarrow \text{Var}\left(\sum_{k=1}^5 A_{2k-1}\right) = 0.0004 \text{ pu}^2 \Rightarrow \sum_{i=1}^5 \sum_{j=1}^5 \text{Cov}(A_{2i-1}, A_{2j-1}) = 0.0004 \text{ pu}^2 \quad (53)$$

From (32), the variance of the measurement vector of the applied Kalman filter can be obtained as

$$\text{Var}(Z) = \text{Var}\left(\sum_{k=1}^5 \lambda_{2k-1} A_{2k-1} + v_d\right) = \sum_{i=1}^5 \sum_{j=1}^5 \lambda_{2i-1} \lambda_{2j-1} \text{Cov}(A_{2i-1}, A_{2j-1}) \quad (54)$$

Although the variance of  $Z$  is not equal to the variance of  $y$ , their per-unit values are the same as their base values acquire the same coefficient, expressed as  $\lambda_{2i-1}\lambda_{2j-1}$  in (54). Therefore, we get

$$\begin{aligned} Var(Z)_{pu} &= \left[ \sum_{i=1}^5 \sum_{j=1}^5 \lambda_{2i-1}\lambda_{2j-1} Cov(A_{2i-1}, A_{2j-1}) \right]_{pu} = \left[ \sum_{i=1}^5 \sum_{j=1}^5 Cov(A_{2i-1}, A_{2j-1}) \right]_{pu} \\ &= Var(y)_{pu} = 0.0004 pu^2 \Rightarrow \sigma_Z = 0.02 pu \Rightarrow R = 0.02^2 = 0.0004 pu^2 \end{aligned} \quad (55)$$

Since the initial state of the sinusoidal components of the signal can be any value between  $+\lambda_{2k-1}a_{2k-1}$  and  $-\lambda_{2k-1}a_{2k-1}$ , the initial state estimate is conservatively assumed to be set at zero for every sinusoidal component. Also, the initial estimate of offset is supposed to be zero. Thus,

$$\hat{X}_0^- = [0, 0, 0, 0, 0, 0, 0, 0, 0, 0]^T \quad (56)$$

Therefore, the initial estimation error covariance matrix can be obtained in the following manner [22].

$$P_0^- = E \left[ (X_0 - \hat{X}_0^-)(X_0 - \hat{X}_0^-)^T \right] = E(X_0 X_0^T) \quad (57)$$

From (19), (26) and (57) the diagonal and non-diagonal elements of  $P_0^-$  can be obtained as follows.

$$P_0^-(i, i) = \begin{cases} E[\lambda_i^2 a_i^2 \cos^2(i\omega t + \theta_i)] & \text{if "i" is odd and } i < 11 \\ E[\lambda_{i-1}^2 a_{i-1}^2 \sin^2[(i-1)\omega t + \theta_{i-1}]] & \text{if "i" is even} \\ E[(2n+1)^2 v_d^2] & \text{if } i = 11 \end{cases} \quad (58)$$

$$P_0^-(i, j) = \begin{cases} E[\lambda_i \lambda_j a_i a_j f(i, j)] & \text{if } i, j < 11 \\ E[\lambda_i a_i (2n+1) v_d g(i)] & \text{if } j = 11 \\ E[\lambda_j a_j (2n+1) v_d g(j)] & \text{if } i = 11 \end{cases} \quad (59)$$

where  $f(i, j)$ ,  $g(i)$  and  $g(j)$  are sinusoidal functions produced due to the existence of sinusoidal parts in the signal components as per (19) and (26). For example,

$$f(3, 6) = \cos(3\omega t + \theta_3) \sin(5\omega t + \theta_5) \quad g(9) = \cos(9\omega t + \theta_9) \quad (60)$$

Since signal is uniformly distributed and  $f$  and  $g$  are purely sinusoidal functions, the average of non-diagonal elements in  $X_0 X_0^T$  will be zero.

From (58), we get

$$P_0^-(i, i) = \begin{cases} E \left[ \frac{\lambda_i^2 a_i^2}{2} + \frac{\lambda_i^2 a_i^2}{2} \cos(2i\omega t + 2\theta_i) \right] & \text{if "i" is odd and } i < 11 \\ E \left[ \frac{\lambda_{i-1}^2 a_{i-1}^2}{2} - \frac{\lambda_{i-1}^2 a_{i-1}^2}{2} \cos[2(i-1)\omega t + 2\theta_{i-1}] \right] & \text{if "i" is even} \\ (2n+1)^2 v_d^2 & \text{if } i = 11 \end{cases} \quad (61)$$

$$P_0^-(i, i) = \begin{cases} \frac{\lambda_i^2 a_i^2}{2} & \text{if "i" is odd and } i < 11 \\ \frac{\lambda_{i-1}^2 a_{i-1}^2}{2} & \text{if "i" is even} \\ (2n+1)^2 v_d^2 & \text{if } i = 11 \end{cases} \quad (62)$$

For the simulations of this paper, the initial estimate covariance matrix is built based on the assumption that the input signal has  $1pu$  of the fundamental component and  $0.01pu$  of odd harmonics up to the ninth order and  $0.05pu$  of offset. Therefore, from (62) the initial estimation error covariance matrix can be stated as follows.

$$P_0^- = \text{diag}. [0.5, 0.5, 0.5 \times 10^{-4}, 0.5 \times 10^{-4}, \dots, 0.5 \times 10^{-4}, 2.5 \times 10^{-3}] pu^2 \quad (63)$$

## References

- [1] M. M. Begovic, P. M. Djuric, S. Dunlap, A. G. Phadke, "Frequency tracking in power networks in the presence of harmonics," IEEE Transactions on Power Delivery, Vol. 8, pp. 480-486, April 1993.
- [2] A. G. Phadke, J. S. Thorp, M. G. Adamiak, "A new measurement technique for tracking voltage phasors, local system frequency, and rate of change of frequency," IEEE Transactions on Power Apparatus and Systems vol. 102, pp. 1025-1038, May 1983.

- [3] J. Yang and C. Liu, "A precise calculation of power system frequency," *IEEE Transaction on Power Delivery*, vol. 16, pp. 361-366, July 1993.
- [4] P. K. Dash, A. K. Pradhan, G. Panda, "Frequency estimation of distorted power system signals using extended complex Kalman filter," *IEEE Transaction on Power Delivery*, vol. 14, pp. 761-766, July 1999.
- [5] A. Routray, A. K. Pradhan, K. P. Rao, "A novel Kalman filter for frequency estimation of distorted signals in power systems," *IEEE Transactions on Instrumentation and Measurement*, vol. 51, pp. 469-479, June 2002.
- [6] A. A. Girgis, T. L. D. Hwang, "Optimal estimation Of voltage phasors and frequency deviation using linear and non-linear Kalman filtering: theory and limitations," *IEEE Transactions on Power Apparatus and Systems*, vol. PAS-103, pp. 2946-2951, Oct. 1984.
- [7] P. J. Moore, R. D. Carranza, A. T. Johns, "A new numeric technique for high-speed evaluation of power system frequency," *IEE Proceedings on Generation, Transmission and Distribution*, vol. 141, pp. 529-536, Sept. 1994.
- [8] M. S. Sachdev, M. M. Giray, "A new numeric technique for high-speed evaluation of power system frequency," *IEEE Transactions on Power Apparatus and Systems*, vol. PAS-104, pp. 437-444, Feb. 1985.
- [9] M. M. Giray, M. S. Sachdev, "Off-nominal frequency measurements in electric power systems," *IEEE Transactions on Power Delivery*, vol. 4, pp. 1573-1578, July 1989.
- [10] V. V. Terzija, M. B. Djuric, B. D. Kovacevic, "Voltage phasor and local system frequency estimation using Newton type algorithm," *IEEE Transactions on Power Delivery*, vol. 9, pp. 1368-1374, July 1994.
- [11] P.K. Dash, B. R. Mishra, R. K. Jena, A. C. Liew, "Estimation of power system frequency using adaptive notch filters," *International Conference on Energy Management and Power Delivery*, 1998. Proceedings of EMPD '98. 1998, vol. 1, pp. 143-148, March 1998.
- [12] H. Karimi, M. Karimi-Ghartemani, M. R. Iravani, "Estimation of frequency and its rate of change for applications in power systems," *IEEE Transactions on Power Delivery*, vol. 19, pp. 472-480, April 2004.
- [13] D. W. P. Thomas, M. S. Woolfson, "Evaluation of frequency tracking methods," *IEEE Transaction on Power Delivery*, vol. 16, pp. 367-371, July 2001.
- [14] R. Aghazadeh, H. Lesani, M. Sanaye-Pasand, B. Ganji, "New technique for frequency and amplitude estimation of power system signals," *IEE Proceedings on Generation, Transmission and Distribution*, vol. 152, pp. 435-440, May 2005.
- [15] S. -K Chung, "Phase-locked loop for grid-connected three-phase power conversion systems," *IEE Proceedings on Electric Power Applications*, vol. 147, pp. 213-219, May 2000.
- [16] M. Karimi-Ghartemani, H. Karimi, A. R. Bakhshai, "A Filtering Technique for Three-Phase Power Systems," *Proceedings of the IEEE Instrumentation and Measurement Technology Conference*, 2005. IMTC 2005, vol. 2, pp. 1503-1506, May 2005.
- [17] M. Karimi-Ghartemani, "A novel three-phase magnitude-phase-locked loop system," *IEEE Transactions on Circuits and Systems I: Regular Papers*, [Circuits and Systems I: Fundamental Theory and Applications], vol. 53, pp. 1792-1802, Aug. 2006.
- [18] M. Karimi-Ghartemani, M. R. Iravani, "A nonlinear adaptive filter for online signal analysis in power systems: applications," *IEEE Transactions on Power Delivery*, vol. 17, pp. 617-622, April 2002.
- [19] M. Karimi-Ghartemani, H. Karimi, M. R. Iravani, "A magnitude/phase-locked loop system based on estimation of frequency and in-phase/quadrature-phase amplitudes," *IEEE Transactions on Industrial Electronics*, vol. 51, pp. 511-517, April 2004.
- [20] M. Sanaye-pasand, R. Aghazadeh, "A new technique for frequency estimation of distorted power system signals," *International Power System Protection Conference (PSP2002)*, Slovenia, September 2002.
- [21] B. D. O. Anderson, J. B. Moore, "Optimal Filtering," (Prentice-Hall, Inc., 1979).
- [22] R. G. Brown, "An introduction to random signal analysis and Kalman filtering," (John Wily & Sons, 1983).